

V. CONCLUSION

The characteristics of the waves guided along a plane interface which separates a semi-infinite region of free space from that of a magnetoionic medium are investigated for the case in which the static magnetic field is oriented perpendicular to the plane interface. It is found that surface waves exist only when $\omega_c < \omega_p$ and that also only for angular frequencies which lie between ω_c and $1/\sqrt{2}$ times the upper hybrid resonant frequency. The surface waves propagate with a phase velocity which is always less than the velocity of electromagnetic waves in free space. The attenuation rates normal to the interface of the surface wave fields in both the media are examined. Numerical results of the surface wave characteristics are given for one typical case.

REFERENCES

- [1] P. S. Epstein, "On the possibility of electromagnetic surface waves," *Proc. Nat'l Acad. Sciences*, vol. 40, pp. 1158-1165, December 1954.
- [2] T. Tamir and A. A. Oliner, "The spectrum of electromagnetic waves guided by a plasma layer," *Proc. IEEE*, vol. 51, pp. 317-332, February 1963.
- [3] M. A. Gintsburg, "Surface waves on the boundary of a plasma in a magnetic field," *Rasprost. Radiovoln i Ionosf., Trudy NIZMIRAN USSR*, no. 17(27), pp. 208-215, 1960.
- [4] S. R. Seshadri and A. Hessel, "Radiation from a source near a plane interface between an isotropic and a gyrotropic dielectric," *Canad. J. Phys.*, vol. 42, pp. 2153-2172, November 1964.
- [5] G. H. Owyang and S. R. Seshadri, "Guided waves propagating along the magnetostatic field at a plane boundary of a semi-infinite magnetoionic medium," *IEEE Trans. on Microwave Theory and Techniques*, vol. MTT-14, pp. 136-144, March 1966.
- [6] S. R. Seshadri and T. T. Wu, "Radiation condition for a magnetoionic medium," to be published.

Numerical Solution of Initial Boundary Value Problems Involving Maxwell's Equations in Isotropic Media

KANE S. YEE

Abstract—Maxwell's equations are replaced by a set of finite difference equations. It is shown that if one chooses the field points appropriately, the set of finite difference equations is applicable for a boundary condition involving perfectly conducting surfaces. An example is given of the scattering of an electromagnetic pulse by a perfectly conducting cylinder.

INTRODUCTION

SOLUTIONS to the time-dependent Maxwell's equations in general form are unknown except for a few special cases. The difficulty is due mainly to the imposition of the boundary conditions. We shall show in this paper how to obtain the solution numerically when the boundary condition is that appropriate for a perfect conductor. In theory, this numerical attack can be employed for the most general case. However, because of the limited memory capacity of present day computers, numerical solutions to a scattering problem for which the ratio of the characteristic linear dimension of the obstacle to the wavelength is large still seem to be impractical. We shall show by an example that in the case of two dimensions, numerical solutions are practical even when the characteristic length of the

obstacle is moderately large compared to that of an incoming wave.

A set of finite difference equations for the system of partial differential equations will be introduced in the early part of this paper. We shall then show that with an appropriate choice of the points at which the various field components are to be evaluated, the set of finite difference equations can be solved and the solution will satisfy the boundary condition. The latter part of this paper will specialize in two-dimensional problems, and an example illustrating scattering of an incoming pulse by a perfectly conducting square will be presented.

MAXWELL'S EQUATION AND THE EQUIVALENT SET OF FINITE DIFFERENCE EQUATIONS

Maxwell's equations in an isotropic medium [1] are:¹

$$\frac{\partial \mathbf{B}}{\partial t} + \nabla \times \mathbf{E} = 0, \quad (1a)$$

$$\frac{\partial \mathbf{D}}{\partial t} - \nabla \times \mathbf{H} = \mathbf{J}, \quad (1b)$$

$$\mathbf{B} = \mu \mathbf{H}, \quad (1c)$$

$$\mathbf{D} = \epsilon \mathbf{E}, \quad (1d)$$

Manuscript received August 24, 1965; revised January 28, 1966. This work was performed under the auspices of the U. S. Atomic Energy Commission.

The author is with the Lawrence Radiation Lab., University of California, Livermore, Calif.

¹ In MKS system of units.

where J , μ , and ϵ are assumed to be given functions of space and time.

In a rectangular coordinate system, (1a) and (1b) are equivalent to the following system of scalar equations:

$$-\frac{\partial B_x}{\partial t} = \frac{\partial E_z}{\partial y} - \frac{\partial E_y}{\partial z}, \quad (2a)$$

$$-\frac{\partial B_y}{\partial t} = \frac{\partial E_x}{\partial z} - \frac{\partial E_z}{\partial x}, \quad (2b)$$

$$\frac{\partial B_z}{\partial t} = \frac{\partial E_y}{\partial x} - \frac{\partial E_x}{\partial y}, \quad (2c)$$

$$\frac{\partial D_x}{\partial t} = \frac{\partial H_z}{\partial y} - \frac{\partial H_y}{\partial z} - J_x, \quad (2d)$$

$$\frac{\partial D_y}{\partial t} = \frac{\partial H_x}{\partial z} - \frac{\partial H_z}{\partial x} - J_y, \quad (2e)$$

$$\frac{\partial D_z}{\partial t} = \frac{\partial H_y}{\partial x} - \frac{\partial H_x}{\partial y} - J_z, \quad (2f)$$

where we have taken $\mathbf{A} = (A_x, A_y, A_z)$. We denote a grid point of the space as

$$(i, j, k) = (i\Delta x, j\Delta y, k\Delta z) \quad (3)$$

and for any function of space and time we put

$$F(i\Delta x, j\Delta y, k\Delta z, n\Delta t) = F^n(i, j, k). \quad (4)$$

A set of finite difference equations for (2a)–(2f) that will be found convenient for perfectly conducting boundary condition is as follows.

For (2a) we have

$$\begin{aligned} & \frac{B_x^{n+1/2}(i, j + \frac{1}{2}, k + \frac{1}{2}) - B_x^{n-1/2}(i, j + \frac{1}{2}, k + \frac{1}{2})}{\Delta t} \\ &= \frac{E_y^n(i, j + \frac{1}{2}, k + 1) - E_y^n(i, j + \frac{1}{2}, k)}{\Delta z} \\ & \quad - \frac{E_z^n(i, j + 1, k + \frac{1}{2}) - E_z^n(i, j, k + \frac{1}{2})}{\Delta y}. \end{aligned} \quad (5)$$

The finite difference equations corresponding to (2b) and (2c), respectively, can be similarly constructed.

For (2d) we have

$$\begin{aligned} & \frac{D_x^n(i + \frac{1}{2}, j, k) - D_x^{n-1}(i + \frac{1}{2}, j, k)}{\Delta t} \\ &= \frac{H_z^{n-1/2}(i + \frac{1}{2}, j + \frac{1}{2}, k) - H_z^{n-1/2}(i + \frac{1}{2}, j - \frac{1}{2}, k)}{\Delta y} \\ & \quad - \frac{H_y^{n-1/2}(i + \frac{1}{2}, j, k + \frac{1}{2}) - H_y^{n-1/2}(i + \frac{1}{2}, j, k - \frac{1}{2})}{\Delta z} \\ & \quad + J_x^{n-1/2}(i + \frac{1}{2}, j, k). \end{aligned} \quad (6)$$

The equations corresponding to (2e) and (2f), respectively, can be similarly constructed.

The grid points for the E -field and the H -field are chosen so as to approximate the condition to be discussed below as accurately as possible. The various grid positions are shown in Fig. 1.

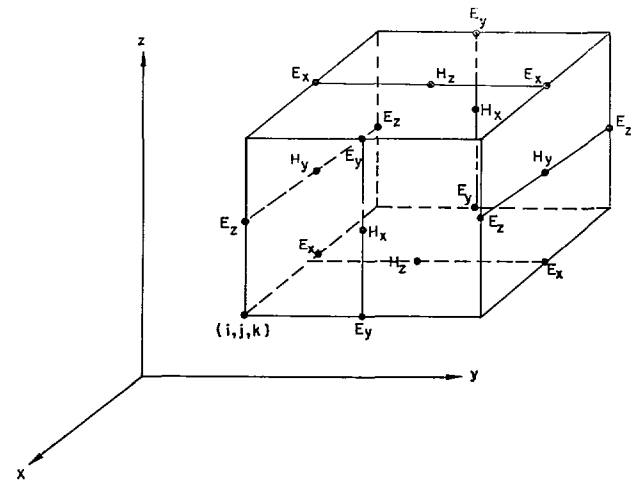


Fig. 1. Positions of various field components. The E -components are in the middle of the edges and the H -components are in the center of the faces.

BOUNDARY CONDITIONS

The boundary condition appropriate for a perfectly conducting surface is that the tangential components of the electric field vanish. This condition also implies that the normal component of the magnetic field vanishes on the surface. The conducting surface will therefore be approximated by a collection of surfaces of cubes, the sides of which are parallel to the coordinate axes. Plane surfaces perpendicular to the x -axis will be chosen so as to contain points where E_y and E_z are defined. Similarly, plane surfaces perpendicular to the other axes are chosen.

GRID SIZE AND STABILITY CRITERION

The space grid size must be such that over one increment the electromagnetic field does not change significantly. This means that, to have meaningful results, the linear dimension of the grid must be only a fraction of the wavelength. We shall choose $\Delta x = \Delta y = \Delta z$. For computational stability, it is necessary to satisfy a relation between the space increment and time increment Δt . When ϵ and μ are variables, a rigorous stability criterion is difficult to obtain. For constant ϵ and μ , computational stability requires that

$$\sqrt{(\Delta x)^2 + (\Delta y)^2 + (\Delta z)^2} > c\Delta t = \sqrt{\frac{1}{\epsilon\mu}} \Delta t, \quad (7)$$

where c is the velocity of light. If c_{\max} is the maximum light velocity in the region concerned, we must choose

$$\sqrt{(\Delta x)^2 + (\Delta y)^2 + (\Delta z)^2} > c_{\max} \Delta t. \quad (8)$$

This requirement puts a restriction on Δt for the chosen Δx , Δy , and Δz .

MAXWELL'S EQUATIONS IN TWO DIMENSIONS

To illustrate the method, we consider a scattering problem in two dimensions. We shall assume that the field components do not depend on the z coordinate of a

point. Furthermore, we take ϵ and μ to be constants and $J \equiv 0$. The only source of our problem is then an "incident" wave. This incident wave will be "scattered" after it encounters the obstacle. The obstacle will be of a few "wavelengths" in its linear dimension. Further simplification can be obtained if we observe the fact that in cylindrical coordinates we can decompose any electromagnetic field into "transverse electric" and "transverse magnetic" fields if ϵ and μ are constants. The two modes of electromagnetic waves are characterized by

1) Transverse electric wave (TE)

$$\begin{aligned} H_x = H_y = 0, \quad E_z = 0, \\ -\mu \frac{\partial H_z}{\partial t} = \frac{\partial E_y}{\partial x} - \frac{\partial E_x}{\partial y}, \\ \epsilon \frac{\partial H_z}{\partial y} = \frac{\partial E_x}{\partial t}, \quad -\frac{\partial H_z}{\partial x} = \epsilon \frac{\partial E_y}{\partial t}, \end{aligned} \quad (9)$$

and

2) Transverse magnetic wave (TM)

$$\begin{aligned} E_x = E_y = 0, \quad H_z = 0, \\ \epsilon \frac{\partial E_z}{\partial t} = \frac{\partial H_y}{\partial x} - \frac{\partial H_x}{\partial y}, \\ \mu \frac{\partial H_x}{\partial t} = -\frac{\partial E_z}{\partial y}, \quad \mu \frac{\partial H_y}{\partial t} = \frac{\partial E_z}{\partial x}. \end{aligned} \quad (10)$$

Let C be a perfectly conducting boundary curve. We approximate it by a polygon whose sides are parallel to the coordinate axes. If the grid dimensions are small compared to the wavelength, we expect the approximation to yield meaningful results.

Letting

$$\tau = ct = \sqrt{\frac{1}{\mu\epsilon}} t \quad (11)$$

and

$$Z = \sqrt{\frac{\mu}{\epsilon}} = 376.7, \quad (12)$$

we can write the finite difference equations for the TE and TM waves.

TE waves:

$$\begin{aligned} H_z^{n+1/2}(i + \frac{1}{2}, j + \frac{1}{2}) = H_z^{n-1/2}(i + \frac{1}{2}, j + \frac{1}{2}) \\ - \frac{1}{Z} \frac{\Delta\tau}{\Delta x} [E_y^n(i + 1, j + \frac{1}{2}) - E_y^n(i, j + \frac{1}{2})] \\ + \frac{1}{Z} \frac{\Delta\tau}{\Delta y} [E_x^n(i + \frac{1}{2}, j + 1) - E_x^n(i + \frac{1}{2}, j)] \end{aligned} \quad (13a)$$

$$E_x^{n+1}(i + \frac{1}{2}, j) = E_x^n(i + \frac{1}{2}, j)$$

$$+ Z \frac{\Delta\tau}{\Delta y} [H_z^{n+1/2}(i + \frac{1}{2}, j + \frac{1}{2}) - H_z^{n+1/2}(i + \frac{1}{2}, j - \frac{1}{2})] \quad (13b)$$

$$\begin{aligned} E_y^{n+1}(i, j + \frac{1}{2}) = -Z \frac{\Delta\tau}{\Delta x} [H_z^{n+1/2}(i + \frac{1}{2}, j + \frac{1}{2}) \\ - H_z^{n+1/2}(i - \frac{1}{2}, j + \frac{1}{2})]. \end{aligned} \quad (13c)$$

TM waves:

$$\begin{aligned} E_z^{n+1}(i, j) = E_z^n(i, j) \\ + Z \frac{\Delta\tau}{\Delta x} [H_y^{n+1/2}(i + \frac{1}{2}, j) - H_y^{n+1/2}(i - \frac{1}{2}, j)] \\ - Z \frac{\Delta\tau}{\Delta y} [H_x^{n+1/2}(i, j + \frac{1}{2}) - H_x^{n+1/2}(i, j - \frac{1}{2})] \end{aligned} \quad (14a)$$

$$\begin{aligned} H_x^{n+1/2}(i, j + \frac{1}{2}) = H_x^{n-1/2}(i, j + \frac{1}{2}) \\ - \frac{1}{Z} \frac{\Delta\tau}{\Delta y} [E_z^n(i, j + 1) - E_z^n(i, j)] \end{aligned} \quad (14b)$$

$$\begin{aligned} H_y^{n+1/2}(i + \frac{1}{2}, j) = H_y^{n-1/2}(i + \frac{1}{2}, j) \\ + \frac{1}{Z} \frac{\Delta\tau}{\Delta x} [E_z^n(i + 1, j) - E_z^n(i, j)]. \end{aligned} \quad (14c)$$

NUMERICAL COMPUTATIONS FOR TM WAVES

For further numerical discussion we shall limit ourselves to the TM waves. In this case we use the finite difference equations (14a)–(14c). The values for $E_z^0(i, j)$, $H_y^{1/2}(i + \frac{1}{2}, j)$, and $H_x^{1/2}(i, j - \frac{1}{2})$ are obtained from the incident wave.² Subsequent values are evaluated from the finite difference equations (14a)–(14c). The boundary condition is approximated by putting the boundary value of $E_z^n(i, j)$ equal to zero for any n .

To be specific, we shall consider the diffraction of an incident TM wave by a perfectly conducting square. The dimensions of the obstacle, as well as the profile of the incident wave, are shown in Fig. 2.

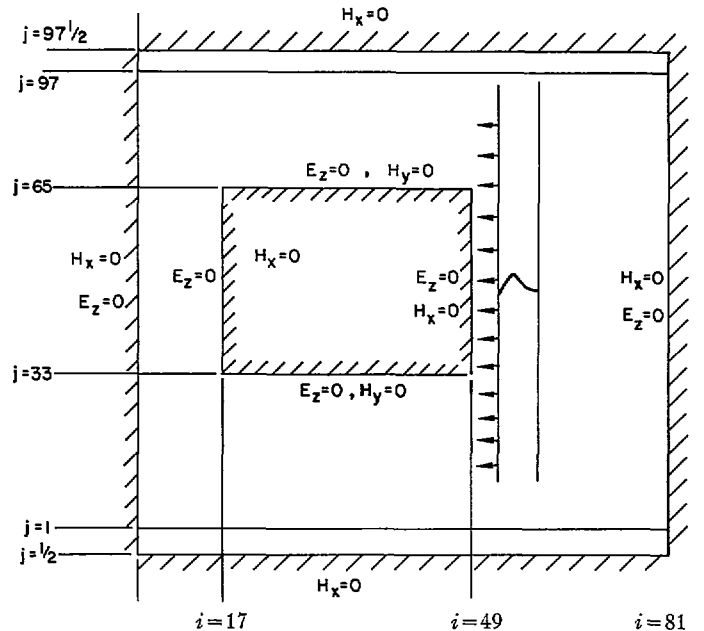


Fig. 2. Equivalent problem for scattering of a TM wave.

² We choose t such that when $t=0$ the incident wave has not encountered the obstacle.

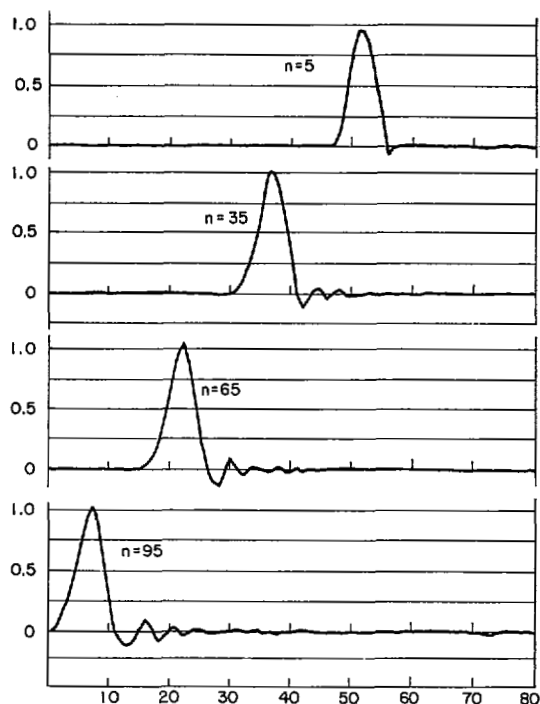


Fig. 3. Results of the calculation of E_z by means of (14a)–(14c) in the absence of the obstacle. The ordinate is in volts/meter and the abscissa is the number of horizontal increments. n is the number of time cycles.

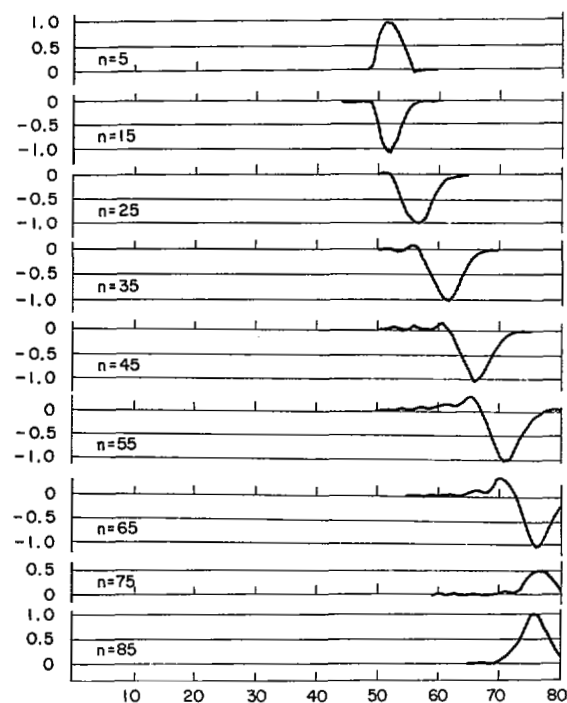


Fig. 5. E_z of the TM wave for various time cycles. $j=50$.

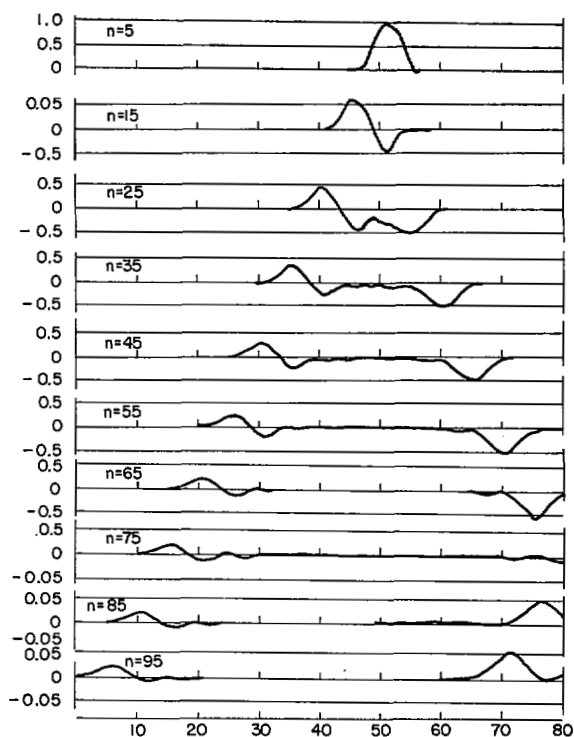


Fig. 4. E_z of the TM wave in the presence of the obstacle for various time cycles when $j=30$.

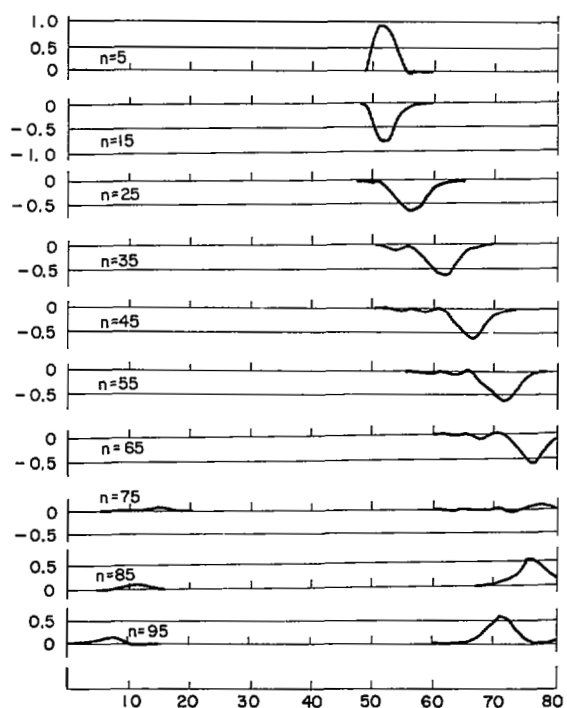


Fig. 6. E_z of the TM wave for various time cycles. $j=65$.

Let the incident wave be plane, with its profile being a half sine wave. The width of the incident wave is taken to be α units and the square has sides of length 4α units. Since the equations are linear, we can take $E_z = 1$ unit. The incident wave will have only an E_z component and an H_y component. We choose

$$\Delta x = \Delta y = \alpha/8 \quad (15a)$$

and

$$\Delta \tau = c\Delta t = \frac{1}{2}\Delta x = \alpha/16. \quad (15b)$$

A finite difference scheme over the whole x - y plane is impractical; we therefore have to limit the extent of our calculation region. We assume that at time $t=0$, the left traveling plane wave is "near" the obstacle. For a restricted period of time, we can therefore replace the original problems by the equivalent problem shown in Fig. 2.

The input data are taken from the incident wave with

$$E_z(x, y, t) = \sin \left[\frac{(x - 50\alpha + ct)\pi}{8\alpha} \right] \\ 0 \leq x - 50\alpha + ct \leq 8\alpha \quad (16a)$$

$$H_y(x, y, t) = \frac{1}{Z} E_z(x, y, t). \quad (16b)$$

From the differential equation satisfied by E_z we conclude that the results for the equivalent problem (see Fig. 2) should approximate those of the original problems, provided

$$0 \leq n\Delta\tau \leq 64\Delta\tau,$$

because the artificial boundary conditions will not affect our solution for this period of time.

For $n > 64$, however, only on certain points will the results of the equivalent problems approximate those of the original problems.

Numerical results are presented for the TM waves discussed above. To gain some idea of the accuracy of the finite difference equation, we have used the system (14a)–(14c) with the initial E_z being a half sine wave for the case of no obstacle. We note that the outer boundary conditions will not affect this incident wave as there is no H_x component in the incident wave. Ninety-five time cycles were run with the finite difference system (14a)–(14c), and the machine output is shown in Fig. 3. The oscillation and the widening of the initial pulse is due to the imperfection of the finite difference system.

Figure 4 shows the value of E_z of the TM wave as a function of the horizontal grid coordinate i for a fixed vertical grid coordinate $j=30$. At the end of five time cycles, the wave just hits the obstacle. The line $j=30$ does not meet the obstacle, but is "sufficiently" near the obstacle to be affected by a "partially reflected" wave. There is also a partially transmitted wave. The phase of the reflected wave is opposite that of the incident wave, as required by the boundary condition of the obstacle. There should also be a decrease in wave amplitude due to cylindrical divergence, but the calcu-

lation was not carried far enough to show this effect.

Figure 5 shows the value of E_z for the TM wave as a function of the horizontal grid coordinate i for $j=50$. This line ($j=50$) meets the obstacle, and hence we expect a reflected wave going to the right. These expectations are borne out in Fig. 5. After the reflected wave from the object meets the right boundary (see Fig. 2), the wave is reflected again. This effect is shown for the time cycles 75, 85, and 95.

Figure 6 is for $j=65$. This line forms part of the boundary of the obstacle. Because of the required boundary condition, E_z is zero on the boundary point. To the right of the obstacle there is a "partially" reflected wave of about half the amplitude of a fully reflected wave. To the left of the obstacle there is a "transmitted" wave after 85 time cycles.

All these graphs were obtained by means of linear interpolation between the grid points. They have been redrawn for reproduction.

COMPARISON OF THE COMPUTED RESULTS WITH THE KNOWN RESULTS ON DIFFRACTION OF PULSES BY A WEDGE

There exist no exact results for the particular example we considered here. However, in the case when the obstacle is a wedge, Keller and Blank [2] and Friedlander [3] have solved the diffraction problem in closed forms. In addition, Keller [4] has also proposed a method to treat diffraction by polygonal cylinders. To carry out the method proposed by Keller [4], one would have to use some sort of finite difference scheme. The present difference scheme seems to be simpler to apply in practice. For a restricted period of time and on a restricted region, our results should be identical with those obtained from diffraction by a wedge. We present such a comparison along the points on the straight line coincident with the upper edge (i.e., $j=65$).

Let the sides of a wedge coincide with the rays $\theta=0$ and $\theta=\beta$. Let the physical space be $0 < r < \infty$, $0 < \theta < \beta$. Let this wedge be perfectly conducting. If the incident E_z is given by

$$E_z^{\text{inc}} = f \left\{ t + \frac{r}{c} \cos(\theta - \theta_0) \right\},$$

where θ_0 is the direction of incidence, Friedlander [3] has shown that the solution to this diffraction problem is

$$E_z(r, \theta, t) = \sigma(\theta - \theta_0) f \left\{ t + \frac{r}{c} \cos(\theta - \theta_0) \right\} \\ - \sigma(\theta + \theta_0) f \left\{ t + \frac{r}{c} \cos(\theta + \theta_0) \right\}^* \\ - \frac{1}{2\beta} \int_0^\infty \{ Q(\theta - \theta_0, \xi) - Q(\theta + \theta_0, \xi) \} \\ \cdot f \left(t - \frac{r}{c} \cosh \xi \right) d\xi, \quad (17)$$

* $(\theta + \theta_0)^* = (\theta + \theta_0) + 2m\beta$, where m is an integer so chosen that $0 < \theta + \theta_0 + 2m\beta < \beta$.
Authorized licensed use only: All rights reserved. Downloaded on August 27, 2013 at 04:23 UTC from IEEE Xplore. Restrictions apply.

where

$$\begin{aligned}\sigma(\psi) &= 1 \quad (|\psi| < \pi); \\ \sigma(\psi) &= 0 \quad (\pi < |\psi| < \beta); \\ \sigma(\psi + 2\beta) &= \sigma(\psi)\end{aligned}$$

and

$$\begin{aligned}k &= \frac{\pi}{\beta} \\ Q(\psi, \xi) &= -\frac{\sin k(\pi + \psi)}{\cosh k\xi - \cos k(\pi + \psi)} \\ &\quad - \frac{\sin k(\pi - \psi)}{\cosh k\xi - \cos k(\pi - \psi)}.\end{aligned}$$

At $t=0$, the incident wave hits the corner.

The discontinuities of the first two terms across the lines $\theta = \theta_0 \pm \pi$ and $\theta = -\theta_0 \pm \pi$ are compensated for by the contributions from the last integral. It can be shown that for

$$\begin{aligned}\theta = \theta_0 &= \frac{\pi}{2}; \quad \beta = \frac{3\pi}{2} \\ E_z\left(r, \frac{\pi}{2}, t\right) &= f\left(t + \frac{r}{2}\right) - \frac{1}{2}f\left(t - \frac{r}{c}\right) \\ &\quad - \frac{\sqrt{3}}{2\pi} \int_0^\infty \frac{f\left(t - \frac{r}{c} \cosh \xi\right)}{\cosh k\xi + \frac{1}{2}} d\xi. \quad (18)\end{aligned}$$

For our incident wave we have⁴

⁴ The origin of the wedge is taken to be the upper right-hand corner of the square. The zero time here differs from that of the numerical integration.

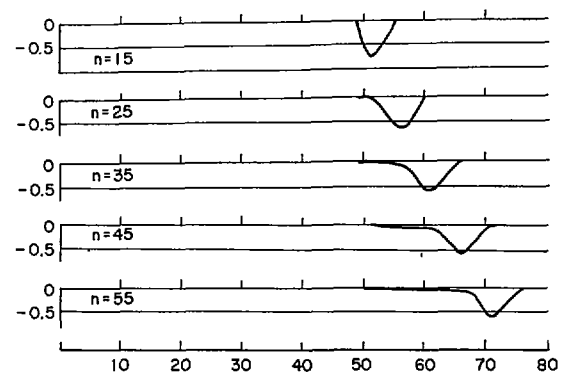


Fig. 7. Calculation of E_z for various cycles. These results are based on (18). The origin of the coordinate and of the time have been adjusted to agree with that used in the numerical calculation.

$$f(t) = \begin{cases} 0 < \frac{c\pi t}{\alpha} < 8 \\ 0 & \text{otherwise.} \end{cases}$$

Results of the computations based on (18) are shown in Fig. 7. The agreement with the graphs on Fig. 6 appears to be good, even for this coarse grid spacing.

ACKNOWLEDGMENT

The author wishes to thank Dr. C. E. Leith for helpful discussions and to express his gratitude to H. Barnett and W. P. Crowley for their assistance in the course of making the numerical calculations.

REFERENCES

- [1] J. Stratton, *Electromagnetic Theory*. New York: McGraw-Hill, 1941, p. 23.
- [2] J. B. Keller and A. Blank, "Diffraction and reflection of pulses by wedges and corners," *Commun. Pure Appl. Math.*, vol. 4, pp. 75-94, June 1951.
- [3] F. G. Friedlander, *Sound Pulses*. New York: Cambridge, 1958.
- [4] J. B. Keller, *Electromagnetic Waves*. Madison, Wis.: Univ. of Wisconsin Press, 1961.